Catalysis Science & Technology

PAPER

View Article Online
View Journal | View Issue

Cite this: *Catal. Sci. Technol.*, 2016, **6**, 5364

Iron amino-bis(phenolate) complexes for the formation of organic carbonates from CO_2 and oxiranes†

Dalal Alhashmialameer,[a] Julie Collins,[b] Karen Hattenhauer[a] and Francesca M. Kerton*[a]

Received 2nd March 2016,
Accepted 24th March 2016

DOI: 10.1039/c6cy00477f

www.rsc.org/catalysis

A series of iron(III) compounds supported by tetradentate amino-bis(phenolate) ligands were synthesized and characterized using electronic absorption spectroscopy, magnetic moment measurement and MALDI-TOF mass spectrometry. The solid-state structures of **1** and **2** were determined by X-ray diffraction and reveal iron(III) square pyramidal compounds. The complexes were studied as catalysts for the reaction of carbon dioxide and epoxides in the presence of a co-catalyst, under solvent free conditions to yield cyclic carbonates. Catalytic testing with TBAB as a co-catalyst shows that **4** bearing electron withdrawing groups in the *ortho* and *para*-positions of the phenolate ring exhibits the highest catalytic activity. Kinetic studies using **1** revealed that the cycloaddition reaction is affected by temperature as expected and the activation energy for propylene carbonate formation is 98.4 kJ mol^{-1}.

Introduction

Utilization of carbon dioxide (CO_2) in the preparation of chemicals with commercial value has become important as it is a green, cheap, non-toxic and abundant feedstock.[1–8] Highly reactive substrates such as epoxides allow for the thermodynamic stability of CO_2 to be overcome.[1,2,9] The interest in cyclic carbonates as CO_2-derived molecules is driven by their wide applications as aprotic solvents (including their use to prepare electrolyte solutions in lithium ion batteries) and as starting materials for polycarbonates.[10] Industrially, the production of cyclic carbonates requires demanding reaction conditions such as elevated CO_2 pressures and high temperatures. Therefore, numerous efforts have been devoted to the design of efficient catalysts for this transformation under mild reaction conditions,[10] including catalysts of aluminum,[11–14] chromium,[15–18] cobalt,[17–22] zinc,[23,24] manganese[25] and magnesium.[26] In order to address the potential toxicity associated with some of these metals, iron complexes have been used as a promising class of catalyst. Moreover, compared with some catalysts, because of iron's high natural abundance, they are often cheap and some recent examples have shown exceptional catalytic activity in the conversion of CO_2 and epoxides to carbonates.[27–29]

To date, several iron-based catalysts have shown excellent activity in the production of both cyclic carbonates and polycarbonates.[26–33] A series of dinuclear iron catalysts based on macrocyclic ligands was reported by the Williams group.[27] Their systems were able to catalyze the reaction of CO_2 and epoxide to produce cyclic carbonates or polycarbonates at only 1 atm pressure of CO_2 in the presence of PPNCl as a co-catalyst. In 2011, a mononuclear iron(II)-system based on a tetraamine ligand was able to produce propylene carbonate without the addition of a co-catalyst.[28] Related cycloaddition reactions catalyzed by monometallic and dimetallic iron(III) complexes chelated with amino-triphenolate ligands have been investigated by Kleij and co-workers (Fig. 1).[29] Later, the same iron complexes were shown to have high activity and selectivity in supercritical carbon dioxide (sc-CO_2) for the production of both cyclic carbonate and polycarbonate at 80 °C

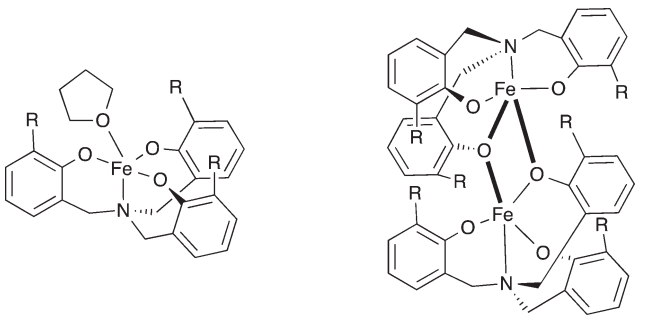

Fig. 1 Monomeric and dimeric iron(III) triphenolate complexes used as a catalyst used by Whiteoak *et al.*[29]

[a] *Department of Chemistry, Memorial University of Newfoundland, St. John's, Newfoundland, A1B 3X7 Canada. E-mail: fkerton@mun.ca*
[b] *C-CART X-ray Diffraction Laboratory, Memorial University of Newfoundland, St. John's, Newfoundland, Canada*

† Electronic supplementary information (ESI) available. CCDC 1452392 and 1452393. For ESI and crystallographic data in CIF or other electronic format see DOI: 10.1039/c6cy00477f

with a strong dependence on co-catalyst loading.[30] In 2013, a new family of ionic monometallic iron(II) and (III) complexes containing N_2O_2 ligands demonstrated high activity for the conversion of CO_2 and epoxide to cyclic carbonates with 99% yield and TON up to 500 without the addition of a co-catalyst.[31] Wang and co-workers have reported very active iron(II) complexes which could catalyze the cycloaddition of CO_2 and epoxides to generate cyclic carbonates with nearly 100% yield and TON of 1000 in 6 h (Fig. 2).[32] Recently, bimetallic iron(III) thioether-triphenolate complexes have shown high activity towards the production of propylene carbonate from the coupling of CO_2 and propylene oxide under solvent-free conditions with the highest reported TON to date, 3480, in only 6 h (Fig. 3).[33] Pescarmona and co-workers reported an effective bifunctional iron(III) pyridylamino-bis(phenolate) complexes FeX[O_2NN′], (X = Cl, Br) to produce either cyclic carbonates (CHC) or polycyclohexene (PCHC) carbonates under solvent free conditions at 60 °C and scCO_2 medium within 18 h.[34]

In the present study, we report the synthesis of new iron(III) complexes supported by tetradentate amino-bis(phenolate) ligands and their catalytic activity for the coupling reaction of CO_2 and various epoxides. Details of the spectroscopic and magnetic properties of these complexes have been included.

Results and discussion

Synthesis and characterization of iron complexes

A series of tetradentate amino-bis(phenol) compounds $H_2[O_2N_2]^{RR'Pip}$ (Fig. 4) were synthesized using a method similar to literature procedures reported by Kerton and co-workers.[35] As shown in Scheme 1, the desired iron(III) complexes were obtained *via* a method reported by Kozak and co-workers,[36] which employs dropwise addition of a methanol solution of anhydrous FeX_3 (X = Cl or Br) to a methanolic slurry of the ligand at room temperature. The resulting solution was neutralized using NEt_3 and evaporated to dryness. Extraction into an appropriate solvent, such as acetone, followed by filtration and removal of the solvent afforded analytically pure paramagnetic complexes with the formulation Fe[L]X.[37–39] The complexes were characterized using MALDI-TOF mass spectrometry, elemental analysis, X-ray diffraction and UV-vis spectroscopy.

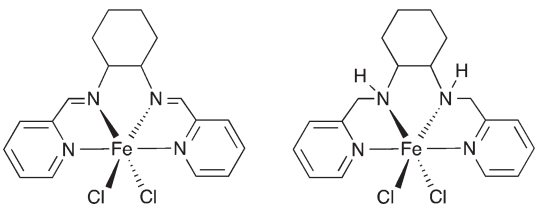

Fig. 2 Iron(II) complexes reported by Sheng *et al.*[32]

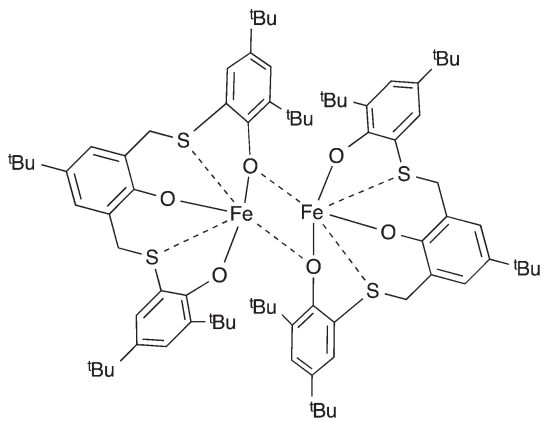

Fig. 3 Bimetallic iron(III) bearing thioether-triphenolate ligands reported by Capacchione, Rieger and co-workers.[33]

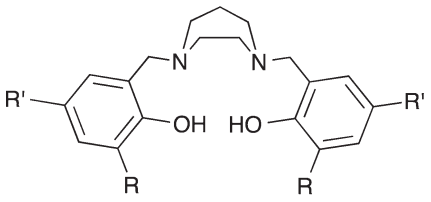

R = R' = tBu (H_2L1)
R = tBu, R '= Me (H_2L2)
R = tBu, R' = OMe (H_2L3)
R = Cl, R' = Cl (H_2L4)

Fig. 4 Proligands used with iron(III) in this study.

Crystal structure determination

Single crystals of **1** and **2** suitable for X-ray diffraction analysis were obtained by slow evaporation and cooling of a saturated methanol or acetone solution at −20 °C. The ORTEP diagrams of the structures are shown in Fig. 5 and S1† and the crystallographic data are collected in Table S1.† Both complexes exhibit monometallic structures with the iron centres bonded to the two phenolate oxygen atoms and two amine nitrogen atoms of the ligand, which define the basal plane of the square pyramid. The apical sites are occupied by chloride ions and the coordination geometry around each iron atom can be described as a distorted square pyramid for both complexes. Selected bond lengths (Å) and angles (°) for compounds **1** and **2** are given in Table S2.† Since both of these complexes are structurally identical except for one substituent, namely a methyl group instead of *tert*-butyl group on the phenolate rings, the observed bond lengths and angles are very similar. For **1**, the phenolate oxygen atoms exhibit bond distances to iron of 1.869(12) and 1.8734(11) Å for Fe–O(1) and Fe–O(2). These Fe–O(1) and Fe–O(2) distances lie within the range observed for **2** [1.8690(12) to 1.8805(12) Å]. These values are similar to those observed in related square pyramidal geometry iron(III) complexes containing salen and bis(phenolate) ligands.[33,40–43] However, they are longer than the corresponding Fe–O bond lengths observed in 5-coordinate iron(III) complexes possessing diamino-bis(phenolate) ligands[38,39,44,45] and salan complexes[46,47] in which the iron(III) ion adopts a trigonal bipyramidal.

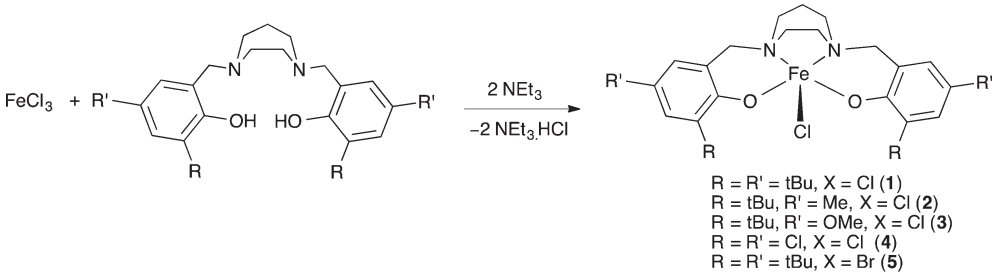

Scheme 1 Synthesis of iron(III) complexes.

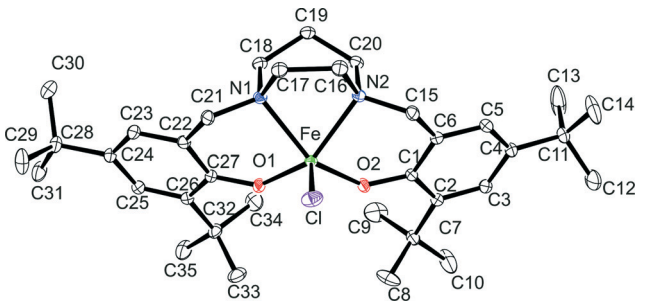

Fig. 5 Molecular structure (ORTEP) and partial numbering scheme for **1**. Ellipsoids are shown at the 50% probability level (H-atoms omitted for clarity).

Moreover, the Fe–O distances are shorter than the average bond length of 1.92 Å observed in octahedral iron(III) complexes,[44,48–51] suggesting relatively strong iron–oxygen overlap which is consistent with the lower coordination number (five rather than six).[44,48] The short Fe–O bond distance is also supported by the high molar absorptivity of the LMCT band (UV-section below). The Fe–Cl(1) distance of 2.2466(6) Å in **1** and 2.2488(8) Å in **2** are shorter than those in the trigonal bipyramidal complexes but similar to the Fe–Cl lengths observed in other square pyramidal iron(III) complexes possessing salen or diamino-bis(phenolate) ligands.[38,40,42,43] The nitrogen donors in the ligand backbone exhibit bond lengths of 2.1864(13) and 2.1681(13) Å for Fe–N(1) and Fe–N(2) in **1**, and lengths of 2.1826(14) and 2.1902(14) Å for Fe–N(1) and Fe–N(2) in **2**. The Fe–N bond distances in both complexes were close to the Fe–N distances in the related square pyramidal complexes.[38,40,42,43] The Fe–O(1)–$C_{(ipso)}$ and Fe–O(2)–$C_{(ipso)}$ in **1** are 138.27(10)° and 137.92(10)° while **2** gives angles of 137.50(10)° and 138.15(10)°, which are identical to those observed in square pyramidal iron(III) complexes of phenolate ligands.[38] The distortion of the coordination around the iron centre was determined by the trigonality parameter τ ($\tau = (\beta - \alpha)/60$), as β the largest angle is O(2)–Fe–N(1) and α the second largest angle in the coordination sphere is O(1)–Fe–N(2).[52] For both complexes, the trigonality index is close to zero.

UV-visible spectroscopic and magnetic data

Based on previous work with iron(III) compounds supported by tetradentate amino-bis(phenolate) ligands, similar electronic absorption spectra were obtained for all of the present complexes.[36,38,50] Since all of these complexes showed similar absorption bands, we can assume that the compounds contain Fe in similar geometries. Complexes **1–5** are intensely purple-coloured solids and their UV-vis spectra exhibit multiple intense bands in the UV and visible regions. Electronic absorption spectra of **1–5** are shown in Fig. 6 and S2–S5.† The highest energy bands (<300 nm) are caused by $\pi \rightarrow \pi^*$ transitions involving the phenolate units. Strong bands in this region are also observed between 330 and 450 nm which are assigned to charge transfer transitions from the out-of-plane pπ orbital (HOMO) of the phenolate oxygen to the half-filled $dx^2\text{-}y^2/dz^2$ orbital of high-spin iron(III). The lowest energy bands (visible region) between 450 and 700 nm arise from charge-transfer transitions from the in-plane pπ orbital of the phenolate to the half-filled dπ* orbital of iron(III) and account for the intense blue/purple colour of the complexes. The halide ligands are anticipated to be labile in solution.[44,50] Changing the halide from chloride to bromide resulted in the lowest energy band appearing at a longer wavelength for the bromide complex compared to the chloride analogue. The lower energy of absorption in **4** (with electron withdrawing groups) reflects the higher Lewis acidity of the iron centre in this complex compared with **1–3** and **5**.

Magnetic susceptibility data for powdered samples were measured at room temperature using a Johnson-Matthey balance. All compounds **1–3** and **5** exhibited moments in the range of 4.6–5.1 μ_B, consistent with high spin d^5 ions.

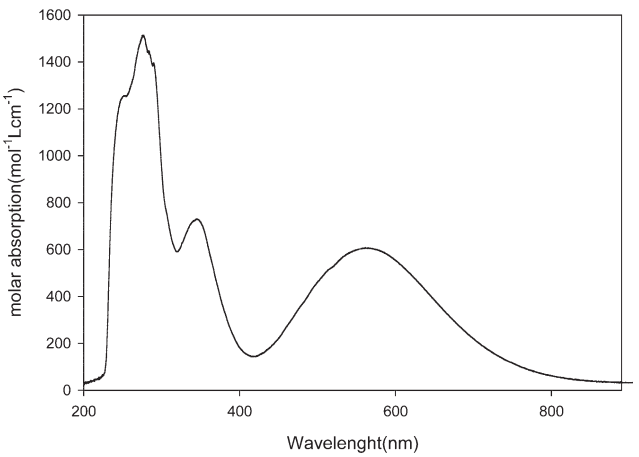

Fig. 6 Electronic absorption spectrum of **1** in dichloromethane.

Complex **4**, however, exhibited a lower magnetic moment than expected (2.3 μ_B) which we postulate is due to the presence of diamagnetic impurities (*e.g.* unreacted ligand), which was confirmed by elemental analysis and MALDI-TOF mass spectrometry. Another possibility for the lower than expected magnetic moment may be spin–spin coupling if a bimetallic complex was formed – however, we observed no peaks for Fe_2-species in the mass spectra of **4**.

Cyclization of propylene oxide with carbon dioxide

Inspired by the promising results reported by the Wang,[32] Capacchione and Rieger[33] groups, complexes **1**–**5** were evaluated as catalysts under similar conditions but longer reaction times. The results are summarized in Table 1. **1** was studied most extensively in order to get baseline results for comparison with other related catalysts. Tetrabutylammonium bromide (TBAB) was used as a co-catalyst and the influence of the reaction temperature, CO_2 pressure and mole ratio of Fe : PO was studied. The presence of the co-catalyst was necessary since no reactivity was observed when catalyst was used alone (entry 1 *vs.* entry 3). Ionic and neutral co-catalysts such as TBAB, bis(triphenylphosphine)iminium chloride (PPNCl), PPN azide ($PPNN_3$) and 4-dimethylaminopyridine (DMAP) were investigated with **1** and compared. The results show that the combination of **1** and TBAB or PPNCl gives the highest activity and conversion compared to other co-catalysts (entries 3 and 5 *vs.* entries 6 and 8). It is well known that the anionic group of the co-catalyst can function as a nucleophile for the ring-opening reaction of the epoxides.[53,54] It should be noted that TBAB and PPNCl salts alone have been reported to yield only small amounts of cyclic carbonate indicating the necessity of an active catalyst for carbonate formation in addition to the ionic co-catalyst.[28,32–34,55] For example, propylene carbonate was produced with a conversion of 33% in the absence of an Fe catalyst in the present student (entry 2). Under the applied conditions, one equivalent of the neutral Lewis base co-catalyst (DMAP) produced only small amounts of propylene carbonate, with an increase to four equivalents inhibiting the reaction (entry 7 *vs.* 8). This can be explained by the ability of DMAP to coordinate to the metal centre which then competes with the incoming epoxide.[1,21] In addition, the ratio between co-catalyst and catalyst was also evaluated under the same conditions using TBAB as the co-catalyst. At higher ratios of co-catalyst, the conversion of cyclic carbonate increased from 63% to 74% which corresponds to an increase in TOF from 115 h^{-1} to 135 h^{-1} (entry 3 *vs.* 9). However, a drop in the conversion and the catalytic activity was observed with further increase of TBAB loading (entry 10). Therefore, all reactions were performed with four equivalents of TBAB.

Cycloadditions, as with many reactions, are strongly influenced by temperature. At elevated temperature (100 °C), a conversion of 74% was reached in 22 h with a corresponding TOF value of 135 h^{-1} (entry 3) confirming the thermal stability of the catalytic system. However, conducting the reaction at room temperature afforded no conversion of PO (entry 11). A similar trend has previously been noted for iron complexes by Wang and co-workers.[32] Therefore, the cycloaddition reaction of PO and CO_2 to form PC typically requires high temperatures and this is in agreement with the fact that selectivity towards formation of the cyclic carbonate product is thermodynamically favored at high temperature. It can also be seen that the pressure of CO_2 has a significant influence on the conversion of PO. When the reaction is conducted at

Table 1 Cycloaddition reactions of propylene oxide and carbon dioxide catalyzed by iron(III) complexes **1**–**5**

Entry[a]	Catalyst	Co-catalyst	[Fe] : [PO] : [Cocat]	Time (h)	T (°C)	Pressure (bar)	Conv. (yield)[h]/%	TON[i]	TOF[j] (h^{-1})
1	**1**	—	1 : 4000 : 0	22	100	20	0	—	—
2	—	TBAB	0 : 4000 : 4	22	100	20	33	1320	60
3	**1**	TBAB	1 : 4000 : 4	22	100	20	74(70)	2960	135
4	**1**	PPNCl	1 : 4000 : 4	6	100	20	27	1080	180
5	**1**	PPNCl	1 : 4000 : 4	22	100	20	70	2800	127
6	**1**	$PPNN_3$	1 : 4000 : 4	22	100	20	18	720	33
7	**1**	DMAP	1 : 4000 : 1	22	100	20	14	560	26
8	**1**	DMAP	1 : 4000 : 4	22	100	20	0	—	—
9[b]	**1**	TBAB	1 : 4000 : 2	22	100	20	63	2520	115
10[c]	**1**	TBAB	1 : 4000 : 10	22	100	20	58	2320	106
11[d]	**1**	TBAB	1 : 4000 : 4	22	25	20	0	—	—
12[e]	**1**	TBAB	1 : 4000 : 4	22	100	40	84	3360	153
13[f]	**1**	TBAB	1 : 4000 : 4	6	100	20	25	1000	167
14[g]	**1**	TBAB	1 : 1000 : 4	22	100	20	58	580	26
15	**2**	TBAB	1 : 4000 : 4	22	100	20	30	1200	55
16	**3**	TBAB	1 : 4000 : 4	22	100	20	34	1360	62
17	**4**	TBAB	1 : 4000 : 4	22	100	20	95	3800	173
18	**5**	TBAB	1 : 4000 : 4	22	100	20	34	1360	62

[a] Reaction conditions (unless otherwise stated): PO (7.0×10^{-2} mol), catalyst (1.75×10^{-5} mol, 0.025 mol%), TBAB (7.0×10^{-5} mol, 0.1 mol%), CO_2 (20 bar); 100 °C, 22 h. [b] Reactions performed with 2 and 10 equivalents of TBAB respectively. [c] Reactions performed with 2 and 10 equivalents of TBAB respectively. [d] Reaction at room temperature. [e] At 40 bar CO_2. [f] 6 h. [g] Reaction conducted with 1000 equivalents of PO. [h] Determined by ^{1}H NMR spectroscopy. [i] Overall turnover number (mol_{PC} mol_{Cat}^{-1}). [j] Overall turnover frequency (TON/reaction time) observed.

20 bar P_{CO_2}, conversion levels of 74% were achieved. At higher pressure, P_{CO_2} = 40 bar, it increased from 74% to 84% (entry 3 *vs.* 12) possibly due to the increased solubility of CO_2 in the epoxide at higher pressure.[2] As expected, the PO conversion was time-dependent as shortening reaction times from 22 h to 6 h led to decreases in the amount of PC obtained (entry 3 and 13, respectively). In addition, the epoxide loading has a significant influence on the reaction course with an increase in conversion being observed with increasing amounts of PO from 1000 to 4000 (entry 14 *vs.* 3, respectively).

The cycloaddition reaction was also tested for complexes **2–5**, in order to identify the most active catalyst and any ligand effects (entries 15–18). As previously reported by others, introducing electron-withdrawing substituents in the *ortho* and *para*-positions of the phenolate ring generates more reactive complexes for the use in the coupling reaction of CO_2 and epoxides.[34,56,57] Our results are in good agreement with this observation as **4** displays the highest catalytic activity with a TOF of 173 h^{-1} (entry 17). A possible explanation is that a decrease in the donor ability of the ligand leads to increased Lewis acidity of the metal centre and enhances the ability of the metal to bind to the epoxide.[1,2] The substitution of the axial ligand by a bromide led to a drop of the catalytic activity with conversions achieving only 34% (entry 18 *cf.* entry 3 for the corresponding chloride complex, conversion 74%). A similar trend was also observed by Pescarmona and co-workers.[34] and they attributed the low activity to the larger radius of bromide which causes steric repulsion for the incoming epoxide substrate when approaching the metal centre. Other reasons for the decrease in activity may be a difference in lability or nucleophilicity of the halide anion. Therefore, overall in the present work activity decreased in the order **4** > **1** > **3** ≥ **5** > **2**. In contrast to the work reported by Pescarmona's group, only a small amount of polypropylene carbonate (4%) could be produced at higher temperature and pressure conditions (70 °C and 70 bar of CO_2).[34]

To expand the scope of the catalytic system, several commercially available epoxides with different electronic and steric properties were examined as substrates using **1** (Table 2). The reaction conditions were chosen according to the conditions presented in Table 1. **1** was able to produce cyclic carbonate from various terminal epoxides containing functional groups. It has recently been noted that the presence of such groups can have a significant effect on the underlying mechanism of the reaction and functional groups such as –OH in glycidol can serve a role in activating carbon dioxide.[58] In our study, epichlorohydrin and glycidol reached conversions higher than those observed for PO (Table 2, entry 1 *vs.* 2 and 3). Such observations have already been documented in earlier studies.[29,32,33,59] Reducing the electron-withdrawing nature of the substituents on the oxirane ring resulted in the production of cyclic carbonate in smaller amounts and low catalytic activity (Table 2, entries 4 and 5). Styrene oxide (SO) exhibited lower reactivity with conversion reaching only 31% (entry 6). This might be due to electronic effects that have been studied computationally, which show that the alkoxide formed from ring-opening of SO is less nucleophilic and therefore less reactive towards carbon dioxide.[60] Further to this, switching the substrate to cyclohexene oxide led to very low conversions compared to all other epoxides used and no polymer was formed (Table 2, entry 7). These results are in

Table 2 Catalytic cyclization of carbon dioxide and epoxides using **1**

Entry[a]	Catalyst	Substrate	Conv.[b]/%	TON[c]	TOF[d] (h^{-1})
1	**1**		74	2960	135
2	**1**		78	3120	142
3	**1**		78	3120	142
4	**1**	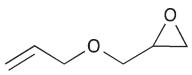	52	2080	95
5	**1**	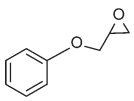	53	2120	96.4
6	**1**	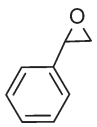	31	1240	57
7	**1**	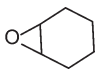	9	364	17

[a] Reaction conditions: substrate (7.0×10^{-2} mol), catalyst (1.75×10^{-5} mol, 0.025 mol%), TBAB (7.0×10^{-5} mol, 0.1 mol%), Fe : [epoxide] : [Cocatalyst] = 1 : 4000 : 4, CO_2 (20 bar); 100 °C, 22 h. [b] Determined by ^{1}H NMR spectroscopy. [c] Overall turnover number (mol_{PC} mol_{Cat}^{-1}). [d] Overall turnover frequency (TON/reaction time) observed.

agreement with the ones reported by the groups of Kleij,[29] Wang,[32] Capacchione and Rieger.[33]

Kinetic measurements

At elevated temperatures, it is known that propylene carbonate is produced as the dominant product in the coupling reaction of PO and CO_2.[19] The production of cyclic carbonates is proposed to occur *via* a backbiting mechanism from either a carbonate or an alkoxide chain end during the coupling process.[19,27] In an effort to better understand the mechanistic aspects of the propylene oxide/carbon dioxide coupling process, a kinetic study for the formation of cyclic propylene carbonate catalyzed by **1** and TBAB was undertaken. Fig. 7 shows the reaction profile obtained using *in situ* infrared spectroscopy. During the course of the reaction, a strong absorption band at 1806 cm^{-1} was seen to increase in intensity and can be assigned to the cyclic carbonate carbonyl group.

Furthermore, as discussed above, temperature has a clear influence on the reaction; therefore, the formation of cyclic carbonate was monitored with respect to increases in temperature (Fig. 8). During the course of the reaction, the temperature was gradually increased and maintained for approximately 25 minutes at each temperature. No cyclic carbonate was observed at room temperature and a small amount formed at 30 and 40 °C. As expected, increasing the temperature further resulted in significant increases in the rate of cyclic carbonate formation. In addition, as shown in the Arrhenius plot (Fig. 9), the activation energy for the formation of the cyclic carbonate could be calculated from the kinetic data. The activation barrier using the **1**/TBAB catalytic system was determined to be 98.4 kJ mol^{-1}, which is in good agreement with the values reported by the groups of Rieger (93.8 kJ mol^{-1}) and Darensbourg (100 kJ mol^{-1}),[28,61] for the cycloaddition of PO with CO_2 using an iron(II) complex containing a tetradentate bis(amino)–bis(pyridyl) ligand and chromium(III) salen complex, respectively. Thus implying that the reaction pathways followed by these catalytic systems are likely very similar.

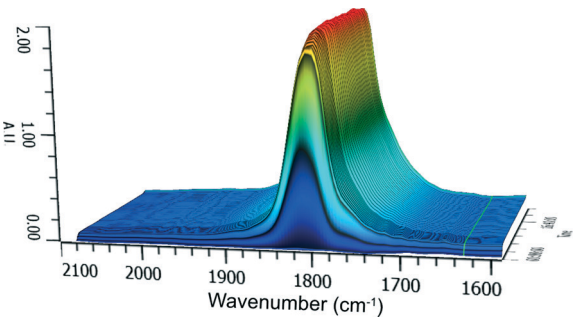

Fig. 7 Three-dimensional stack plots of the IR spectra using **1** at 20 bar, 100 °C and [Fe] : [PO] : [Cocat] 1 : 4000 : 4.

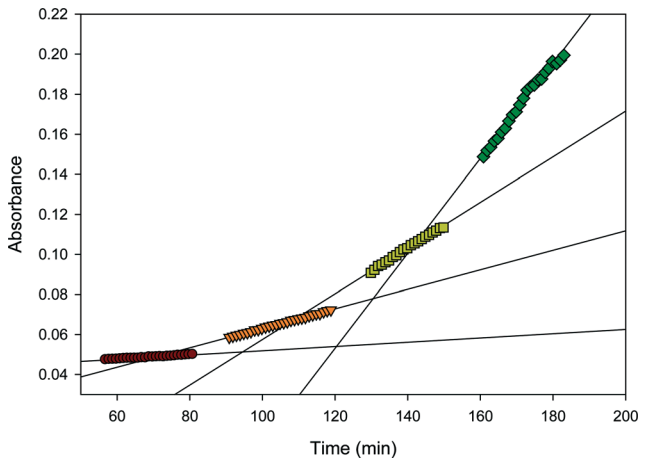

Fig. 8 Initial rates of reaction profile at various temperature based on the absorbance of the ν(C=O) of the propylene carbonate (PC). ● at 50 °C (y = 0.0001066x + 0.04121, R^2 = 0.9838), ▼ at 60 °C (y = 0.0004866x + 0.01444, R^2 = 0.9987), ■ at 70 °C (y = 0.001141x − 0.05657, R^2 = 0.9971), ◆ at 80 °C (y = 0.002372x − 0.2107, R^2 = 0.988).

Conclusions

New air stable iron(III) complexes based on amino-bis(phenolate) ligands were prepared and characterized. The structures of **1** and **2** were determined and reveal iron(III) centres in square pyramidal environments. The complexes in combination with TBAB exhibit promising activity towards the catalytic formation of cyclic carbonates. It was found that the presence of electron withdrawing groups in the *ortho*- and *para*-positions of the phenolate rings increases the reactivity of catalysts. On the basis of the kinetic data at different temperatures, the activation energy determined for cyclic carbonate formation was close to those previously reported.

Experimental

General experimental conditions

Reagents were purchased from either Sigma-Aldrich or Alfa Aesar and used without further purification. Commercially available solvents were used without further purification. Reactions for synthesizing ligands and iron complexes were

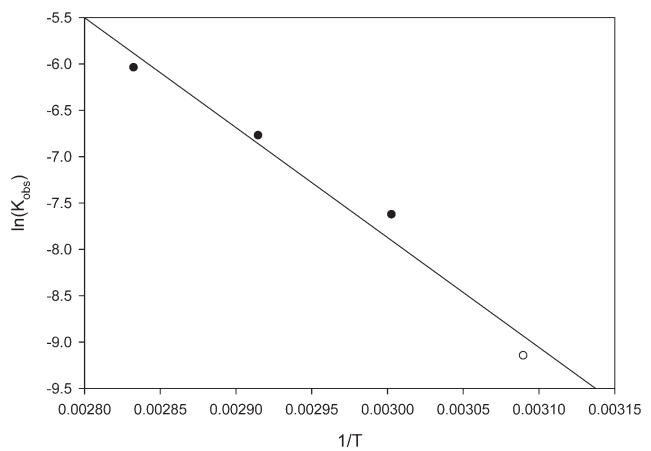

Fig. 9 Arrhenius plot for the formation of PC. Straight line: y = −11 840x + 27.25, R^2 = 0.9713.

performed in air. H_2L1 and H_2L2 were prepared using a previously described procedure.[62]

Instrumentation

^1H and $^{13}C\{^1H\}$ NMR spectra were recorded on a Bruker Avance 300 MHz spectrometer at 25 °C and were referenced internally using the residual proton and ^{13}C resonances of the solvent. MALDI-TOF MS spectra were obtained using an Applied Biosystems 4800 MALDI TOF/TOF Analyzer equipped with a reflectron, delayed ion extraction and high performance nitrogen laser (200 Hz operating at 355 nm). Samples were prepared at a concentration of 10.0 mg mL^{-1} in toluene. Matrix (anthracene) was mixed at a concentration of 10.0 mg mL^{-1} to promote desorption and ionization. Separate vials were used to mix 20 μL of the sample solution with 20 μL of the matrix solution. 1 μL of the sample and matrix mixture were spotted on a MALDI plate and left to dry. Images of mass spectra were prepared using mMass™ software (www.mmass.org). The crystal structures were collected on a AFC8-Saturn 70 single crystal X-ray diffractometer from Rigaku/MSC, equipped with an X-stream 2000 low temperature system (CCDC numbers: 1452392 and 1452393). UV-vis spectra were recorded on an Ocean Optics USB4000+ fiber optic spectrophotometer. The room temperature magnetic measurements were obtained using a Johnson-Matthey magnetic susceptibility balance. The data were corrected for the diamagnetism of all atoms and the balance was calibrated using $Hg[Co(NCS)_4]$. In addition to reactions described below that use a 100 mL pressure vessel equipped for IR-monitoring, cycloaddition reactions were also carried out in a 300 mL stainless steel Parr® 5500 autoclave reactor with a Parr® 4836 controller.

In situ monitoring of the cycloaddition reaction by IR spectroscopy

In situ monitoring was carried out using a modified 100 mL stainless steel reactor vessel (Parr Instrument Company) equipped with a silicon sensor (SiComp), motorized mechanical stirrer and a heating mantle. The silicon sensor was connected to a ReactIR 15 base unit (Mettler-Toledo) through a DS silver-halide Fiber-to-Sentinel conduit. The reactor vessel was cleaned and heated under vacuum at 80 °C overnight before experiments. The appropriate amount of complex and co-catalyst were weighed and then dissolved in 4 g PO which afforded a purple solution. The mixture was stirred for about 10 min and the reaction solution was transferred into a 5 mL syringe with a cannula needle attached. The syringe was injected into the vessel through a port. Then the vessel was pressurized with 20 bar CO_2. Heating and stirring were started and the reaction was monitored for the allotted time. After venting the reaction vessel, it was noted that the mixture had changed colour – a brown solution had formed.

Synthesis and characterization of ligands and catalysts

Synthesis of $[H_2L3]$. A mixture of 3-*tert*-butyl-4-hydroxyanisole (24.4 g, 0.123 mol), 37% w/w formaldehyde (10.0 mL, 0.123 mol) and homopiperazine (6.22 g, 0.0615 mol) in water (100 mL) was stirred and heated to reflux for 24 h. Upon cooling to room temperature, solvents were decanted from the resulting white solid, which was recrystallized from methanol and chloroform to afford a pure white powder (24 g, 85.7%). ^1H NMR (300 MHz, 298 K, $CDCl_3$) δ 10.72 (2H, s, O*H*), 6.80 (2H, d, $^2J_{HH}$ = 2.6, Ar*H*), 6.40 (2H, d, $^2J_{HH}$ = 2.6, Ar*H*), 3.73 (4H, s, ArC–CH_2–N), 3.48 (6H, s, ArC–OCH_3), 2.81 (4H, t, $^3J_{HH}$ = 6.1 Hz, N–CH_2CH_2–N), 2.76 (4H, br, N–CH_2{CH_2}CH_2–N), 1.88 (2H, quintet, $^3J_{HH}$ = 6.01 Hz, N–CH_2{CH_2}CH_2–N), 1.4 (18H, s, ArC–C(CH_3)$_3$). $^{13}C\{^1H\}$ NMR (300 MHz, 298 K, $CDCl_3$) δ 151.8 (Ar*C*–O), 150.6 (Ar*C*–OCH$_3$), 138.0 (Ar*C*–C(CH$_3$)$_3$), 122.0 (Ar*C*H), 112.8 (Ar*C*H), 111.2 (Ar*C*–CH$_2$–N), 62.2 (ArC–*C*H$_2$–N), 55.7 (ArC–O*C*H$_3$), 54.5 (N–*C*H$_2${CH$_2$}*C*H$_2$–N), 53.0 (N–*C*H$_2$*C*H$_2$–N), 34.9 (ArC–*C*–(CH$_3$)$_3$), 29.4 (ArC–C–(*C*H$_3$)$_3$), 26.8 (N–CH$_2${*C*H$_2$}CH$_2$–N). MS (MALDI-TOF) *m*/*z* (%, ion): 484.3 (100, $H_2[N_2O_2{}^{BuOMePip}]^{\bullet+}$).

Synthesis of $[H_2L4]$. A mixture of 2,4-dichlorophenol (24.4 g, 0.123 mol), 37% w/w formaldehyde (10.0 mL, 0.123 mol) and homopiperazine (6.22 g, 0.0615 mol) in water (50 mL) was stirred and heated to reflux for 72 h. Upon cooling to room temperature, solvents were decanted from the resulting yellow solid (18.5 g, 67%). ^1H NMR (300 MHz, 298 K, $CDCl_3$) δ 11.65 (2H, s, O*H*), 7.24 (2H, d, $^2J_{HH}$ = 2.3 Hz, Ar*H*), 6.84 (2H, d, $^2J_{HH}$ = 2.3 Hz, Ar*H*), 3.75 (4H, s, ArC–CH_2–N), 2.83 (4H, t, $^3J_{HH}$ = 6 Hz, N–CH_2CH_2–N), 2.79 (4H, s, N–CH_2{CH$_2$}CH_2–N), 1.97 (2H, quintet, $^3J_{HH}$ = 6.04 Hz, N–CH$_2${CH_2}CH$_2$–N). $^{13}C\{^1H\}$ NMR (300 MHz, 298 K, $CDCl_3$) δ 152.40 (Ar*C*–O), 128.70 (Ar*C*Cl), 126.51 (Ar*C*Cl), 123.43 (Ar*C*H), 123.31 (Ar*C*H), 121.37 (Ar*C*–CH$_2$–N), 61.11 (ArC–*C*H$_2$–N), 54.05 (N–*C*H$_2${CH$_2$}*C*H$_2$–N), 25.97 (N–CH$_2${*C*H$_2$}CH$_2$–N). MS (MALDI-TOF) *m*/*z* (%, ion): 449 (100, $H_2[N_2O_2{}^{ClClPip}]^{\bullet+}$).

Synthesis of 1. To a methanol solution (30 mL) of recrystallized H_2L1 (2.52 g, 4.7 mmol) was added a solution of anhydrous $FeCl_3$ (0.762 g, 4.7 mmol) in methanol resulting in purple solution. To this solution was added triethylamine (0.819 g, 9.4 mmol) and the resulting mixture was stirred for 2 h. After stirring, the solvent was removed under vacuum. The purple product was dissolved in acetone (50 mL) and filtered through Celite three times. Removal of solvent under vacuum yielded a black powder (2.61 g, 88%). Anal. calc'd for $C_{35}H_{54}FeClN_2O_2{\cdot}C_3H_6O$: C, 66.71; H, 8.84; N, 4.09. Found: C, 66.7; H, 8.80; N, 4.19. MS (MALDI-TOF) *m*/*z* (%, ion): 664.2 (15, $FeClK[N_2O_2{}^{BuBuPip}]^{\bullet+}$), 625.2 (85, $FeCl[N_2O_2{}^{BuBuPip}]^{\bullet+}$), 590.3 (94.3, $Fe[N_2O_2{}^{BuBuPip}]^{\bullet+}$). UV-vis ($CH_2Cl_2$) λ_{max}, nm (ε): 570 nm. μ_{eff} (solid, 25 °C) = 4.68 μ_B.

Synthesis of 2. To a methanol solution (30 mL) of recrystallized H_2L2 (2.51 g, 5.5 mmol) was added a solution of anhydrous $FeCl_3$ (0.899 g, 5.5 mmol) in methanol resulting in an intense purple solution. To this solution was added triethylamine (0.967 g, 11.1 mmol) and the resulting mixture was stirred for 2 h. After stirring, the solvent was removed under vacuum. The purple product was dissolved in acetone (50 mL) and filtered through Celite. Removal of solvent under vacuum yielded a black powder (2.5 g, 86%). Anal. calc'd for $C_{29}H_{42}FeClN_2O_2$: C, 64.27; H, 7.81; N, 5.17. Found: C, 64.14; H, 8.10; N, 5.37. MS (MALDI-TOF) *m*/*z* (%, ion): 580.1 (12.2,

FeClK[$N_2O_2^{BuMePip}$]$^{\bullet+}$), 541.1 (32.4, FeCl[$N_2O_2^{BuMePip}$]$^{\bullet+}$), 506 (63, Fe[$N_2O_2^{BuMePip}$]$^{\bullet+}$). UV-vis (CH_2Cl_2) λ_{max}, nm (ε): 580 nm. μ_{eff} (solid, 25 °C) = 5.1 μ_B.

Synthesis of 3. To a methanol solution (30 mL) of recrystallized **H_2L3** (2.52 g, 5.5 mmol) was added a solution of anhydrous $FeCl_3$ (0.896 g, 5.5 mmol) in methanol resulting in an intense blue solution. To this solution was added triethylamine (0.965 g, 11.1 mmol) and the resulting mixture was stirred for 2 h. After stirring, the solvent was removed under vacuum. The purple product was dissolved in acetone (50 mL) and filtered through Celite. Removal of solvent under vacuum yielded a black powder (2.5 g, 79%). Anal. calc'd for $C_{29}H_{42}FeClN_2O_4{\cdot}C_3H_6O$: C, 60.81; H, 7.66; N, 4.43. Found: C, 60.9; H, 7.41; N, 4.63. MS (MALDI-TOF) *m*/*z* (%, ion): 573.1 (98.6, FeCl[$N_2O_2^{BuOMePip}$]$^{\bullet+}$), 538.2 (43.1, Fe[$N_2O_2^{BuOMePip}$]$^{\bullet+}$). UV-vis (CH_2Cl_2) λ_{max}, nm (ε): 580 nm. μ_{eff} (solid, 25 °C) = 5.1 μ_B.

Synthesis of 4. To a methanol solution (30 mL) of recrystallized **H_2L4** (2.52 g, 5.6 mmol) was added a solution of anhydrous $FeCl_3$ (0.91 g, 5.6 mmol) in methanol resulting in an intense blue solution. To this solution was added triethylamine (0.977 g, 11.2 mmol) and the resulting mixture was stirred for 2 h. After stirring, the solvent was removed under vacuum. The purple product was dissolved in acetone (50 mL) and filtered through Celite. Removal of solvent under vacuum yielded a dark black powder (2.9 g, 82%). Anal. calc'd for $C_{19}H_{18}FeCl_5N_2O_2(1.5CH_3OH)(0.5$**$H_2$L4**$)$: C, 44.34; H, 4.22; N, 5.17. Found: C, 44.48; H, 4.66; N, 5.69. MS (MALDI-TOF) *m*/*z* (%, ion): 538.24 (90, FeCl[$N_2O_2^{ClClPip}$]$^{\bullet+}$), 503.98 (35, Fe[$N_2O_2^{ClClPip}$]$^{\bullet+}$). UV-vis (CH_2Cl_2) λ_{max}, nm (ε): 550 nm. μ_{eff} (solid, 25 °C) = 2.3 μ_B.

Synthesis of 5. To a methanol solution (30 mL) of recrystallized **H_2L1** (2.52 g, 4.7 mmol) was added a solution of anhydrous $FeBr_3$ (1.389 g, 4.7 mmol) in methanol resulting in an intense blue solution. To this solution was added triethylamine (0.819 g, 9.4 mmol) and the resulting mixture was stirred for 2 h. After stirring, the solvent was removed under vacuum. The purple product was dissolved in acetone (50 mL) and filtered through Celite. Removal of solvent under vacuum yielded a dark black powder (2.9 g, 92%). Anal. calc'd for $C_{35}H_{54}FeBrN_2O_2$: C, 62.69; H, 8.12; N, 4.18. Found: C, 62.87; H, 7.97; N, 4.24. MS (MALDI-TOF) *m*/*z* (%, ion): 669.29 (45.5, FeBr[$N_2O_2^{BuBuPip}$]$^{\bullet+}$), 590.38 (81.8, Fe[$N_2O_2^{BuBuPip}$]$^{\bullet+}$). UV-vis (CH_2Cl_2) λ_{max}, nm (ε): 580 nm. μ_{eff} (solid, 25 °C) = 4.85 μ_B.

Spectroscopic data for carbonate products

4-Methyl-1,3-dioxolan-2-one. (Table 2, entry 1).[31,56] ^{1}H NMR (300 MHz, 298 K, $CDCl_3$): δ 4.7 (1H, m, C*H*O), 4.4 (1H, t, $^3J_{HH}$ = 7.1 Hz, OCH_2), 3.8 (1H, t, $^3J_{HH}$ = 7.1 Hz, OCH_2), 1.26 (3H, d, $^3J_{HH}$ = 6 Hz, CH_3). ^{13}C {^{1}H} NMR (300 MHz, 298 K, $CDCl_3$) δ 155 (C–*C*O), 73.5 (C–*C*H), 70.5 (C–*C*H_2), 18.9 (C–*C*H_3).

4-Chloromethyl-1,3-dioxolan-2-one. (Table 2, entry 2).[31,33,56] ^{1}H NMR (300 MHz, 298 K, $CDCl_3$) δ 4.94 (1H, m, C*H*O), 4.54 (1H, t, $^3J_{HH}$ = 8.9 Hz, OCH_2), 4.35 (1H, dd, $^3J_{HH}$ = 9.2 Hz, OCH_2), 3.7–3.9 (2H, m, CH_2Cl). ^{13}C {^{1}H} NMR (300 MHz, 298 K, $CDCl_3$) δ 154.5 (C–*C*O), 74.5 (C–*C*H), 67 (C–*C*H_2Cl), 44.1 (C–*C*H_2).

4-Hydroxymethyl-1,3-dioxolan-2-one. (Table 2, entry 3).[33,56] ^{1}H NMR (300 MHz, 298 K, $CDCl_3$) δ 4.8 (1H, m, C*H*O), 4.4–4.6 (2H, m, OCH_2), 3.6–4.1 (1H, m, CH_2O*H*). ^{13}C {^{1}H} NMR (300 MHz, 298 K, $CDCl_3$) δ 155.6 (C–*C*O), 75.27 (C–*C*H), 66.02 (C–*C*H_2OH), 44.01 (C–*C*H_2).

4-Allyloxymethyl-1,3-dioxolan-2-one. (Table 2, entry 4).[33,56] ^{1}H NMR (300 MHz, 298 K, $CDCl_3$) δ 5.8 (1H, m, C*H*), 5–5.15 (2H, m, CH_2), 4.71 (1H, s, OC*H*), 4.4 (1H, t, $^3J_{HH}$ = 8.5 Hz, OCH_2), 4.2 (1H, dd, $^3J_{HH}$ = 8.5 Hz, OCH_2), 3.9 (2H, d, OCH_2), 3.4–3.6 (2H, m, CH_2O). ^{13}C {^{1}H} NMR (300 MHz, 298 K, $CDCl_3$) δ 155.0 (C–*C*O), 117 (C–CH*C*H_2), 133.7 (C–*C*HCH$_2$), 75.2 (C–*C*H), 72 (C–*C*H_2O), 66.1 (C–*C*H_2O), 44.0 (C–*C*H_2).

4-Phenoxymethyl-1,3-dioxolan-2-one. (Table 2, entry 5).[31,33] ^{1}H NMR (300 MHz, 298 K, $CDCl_3$) δ 7.3 (5H, m, Ar*H*), 5.3 (1H, s, ArC*H*), 5 (1H, m, OC*H*), 4.6 (2H, m, PhCH_2O), 4.2 (2H, m, OCH_2). ^{13}C {^{1}H} NMR (300 MHz, 298 K, $CDCl_3$) δ 155.0 (C–*C*O), 137 (Ar–CO), 121.3 (Ar*C*H_2), 114.7 (Ar–C–*C*H_2), 75.7 (C–*C*H), 66.2 (C–*C*H_2O), 44.8 (C–*C*H_2).

4-Phenyl-1,3-dioxolan-2-one. (Table 2, entry 6).[31,33,56] ^{1}H NMR (300 MHz, 298 K, $CDCl_3$) δ 7.3 (5H, m, Ar*H*), 5.6 (1H, t, $^3J_{HH}$ = 8.2 Hz, ArC*H*), 4.7 (1H, t, $^3J_{HH}$ = 8.7 Hz, OC*H*), 4.2 (2H, t, $^3J_{HH}$ = 8.7 Hz, OCH_2). ^{13}C {^{1}H} NMR (300 MHz, 298 K, $CDCl_3$) δ 154.9 (C–*C*O), 136 (Ar–CO), 128.5 (Ar*C*H_2), 126 (Ar–C–*C*H_2), 71.1 (C–*C*H), 51.1 (C–*C*H_2).

Cis-1,2-cyclohexene carbonate. (Table 2, entry 7).[31,33] ^{1}H NMR (300 MHz, 298 K, $CDCl_3$) δ 2.89 (2H, m, OC*H*CH$_2$CH$_2$), 1.63 (4H, m, OCHC*H*$_2$CH$_2$), 1.20 (2H, m, OCHCH$_2$C*H*$_2$), 1.03 (2H, m, OCHCH$_2$C*H*$_2$). ^{13}C {^{1}H} NMR (300 MHz, 298 K, $CDCl_3$) δ 154.9 (C–*C*O), 75.5 (O*C*HCH$_2$CH$_2$), 26.6 (OCH*C*H$_2$CH$_2$), 19.1 (OCHCH$_2$*C*H$_2$).

Acknowledgements

NSERC of Canada, Memorial University, RDC-NL and CFI are thanked for operating and instrument grants. D. A. gives special thanks to the Saudi Arabian Cultural Bureau in Canada and Taif University (Saudi Arabia) for financial support.

References

1 S. Klaus, M. W. Lehenmeier, C. E. Anderson and B. Rieger, *Coord. Chem. Rev.*, 2011, **255**, 1460–1479.
2 P. P. Pescarmona and M. Taherimehr, *Catal. Sci. Technol.*, 2012, **2**, 2169–2187.
3 T. Sakakura and K. Kohno, *Chem. Commun.*, 2009, 1312–1330.
4 B. Schäffner, F. Schäffner, S. P. Verevkin and A. Börner, *Chem. Rev.*, 2010, **110**, 4554–4581.
5 H. Arakawa, M. Aresta, J. N. Armor, M. A. Barteau, E. J. Beckman, A. T. Bell, J. E. Bercaw, C. Creutz, E. Dinjus, D. A. Dixon, K. Domen, D. L. DuBois, J. Eckert, E. Fujita, D. H. Gibson, W. A. Goddard, D. W. Goodman, J. Keller, G. J.

Kubas, H. H. Kung, J. E. Lyons, L. E. Manzer, T. J. Marks, K. Morokuma, K. M. Nicholas, R. Periana, L. Que, J. Rostrup-Nielson, W. M. H. Sachtler, L. D. Schmidt, A. Sen, G. A. Somorjai, P. C. Stair, B. R. Stults and W. Tumas, *Chem. Rev.*, 2001, **101**, 953–996.
6 A. I. Cooper, *J. Mater. Chem.*, 2000, **10**, 207–234.
7 H. Yasuda, L.-N. He, T. Sakakura and C. Hu, *J. Catal.*, 2005, **233**, 119–122.
8 O. V. Zalomaeva, A. M. Chibiryaev, K. A. Kovalenko, O. A. Kholdeeva, B. S. Balzhinimaev and V. P. Fedin, *J. Catal.*, 2013, **298**, 179–185.
9 D. J. Darensbourg and M. W. Holtcamp, *Coord. Chem. Rev.*, 1996, **153**, 155–174.
10 M. North, R. Pasquale and C. Young, *Green Chem.*, 2010, **12**, 1514–1539.
11 X.-B. Lu, Y.-J. Zhang, B. Liang, X. Li and H. Wang, *J. Mol. Catal. A: Chem.*, 2004, **210**, 31–34.
12 G. A. Luinstra, G. R. Haas, F. Molnar, V. Bernhart, R. Eberhardt and B. Rieger, *Chem. – Eur. J.*, 2005, **11**, 6298–6314.
13 S. H. Kim, D. Ahn, M. J. Go, M. H. Park, M. Kim, J. Lee and Y. Kim, *Organometallics*, 2014, **33**, 2770–2775.
14 I. S. Metcalfe, M. North and P. Villuendas, *J. CO_2 Util.*, 2013, **2**, 24–28.
15 S. Iksi, A. Aghmiz, R. Rivas, M. D. González, L. Cuesta-Aluja, J. Castilla, A. Orejón, F. El Guemmout and A. M. Masdeu-Bultó, *J. Mol. Catal. A: Chem.*, 2014, **383–384**, 143–152.
16 Y. Niu, W. Zhang, H. Li, X. Chen, J. Sun, X. Zhuang and X. Jing, *Polymer*, 2009, **50**, 441–446.
17 M. Adolph, T. A. Zevaco, C. Altesleben, O. Walter and E. Dinjus, *Dalton Trans.*, 2014, **43**, 3285–3296.
18 M. Sunjuk, A. Abu-Surrah, E. Al-Ramahi, A. Qaroush and A. Saleh, *Transition Met. Chem.*, 2013, **38**, 253–257.
19 X.-B. Lu and D. J. Darensbourg, *Chem. Soc. Rev.*, 2012, **41**, 1462–1484.
20 L. N. Saunders, N. Ikpo, C. F. Petten, U. K. Das, L. N. Dawe, C. M. Kozak and F. M. Kerton, *Catal. Commun.*, 2012, **18**, 165–167.
21 R. L. Paddock, Y. Hiyama, J. M. McKay and S. T. Nguyen, *Tetrahedron Lett.*, 2004, **45**, 2023–2026.
22 K. L. Peretti, H. Ajiro, C. T. Cohen, E. B. Lobkovsky and G. W. Coates, *J. Am. Chem. Soc.*, 2005, **127**, 11566–11567.
23 A. Decortes, M. Martinez Belmonte, J. Benet-Buchholz and A. W. Kleij, *Chem. Commun.*, 2010, **46**, 4580–4582.
24 S.-i. Fujita, M. Nishiura and M. Arai, *Catal. Lett.*, 2010, **135**, 263–268.
25 P. Ramidi, C. M. Felton, B. P. Subedi, H. Zhou, Z. R. Tian, Y. Gartia, B. S. Pierce and A. Ghosh, *J. CO_2 Util.*, 2015, **9**, 48–57.
26 C.-Y. Li, C.-R. Wu, Y.-C. Liu and B.-T. Ko, *Chem. Commun.*, 2012, **48**, 9628–9630.
27 A. Buchard, M. R. Kember, K. G. Sandeman and C. K. Williams, *Chem. Commun.*, 2011, **47**, 212–214.
28 J. E. Dengler, M. W. Lehenmeier, S. Klaus, C. E. Anderson, E. Herdtweck and B. Rieger, *Eur. J. Inorg. Chem.*, 2011, **2011**, 336–343.
29 C. J. Whiteoak, B. Gjoka, E. Martin, M. M. Belmonte, E. C. Escudero-Adán, C. Zonta, G. Licini and A. W. Kleij, *Inorg. Chem.*, 2012, **51**, 10639–10649.
30 M. Taherimehr, S. M. Al-Amsyar, C. J. Whiteoak, A. W. Kleij and P. P. Pescarmona, *Green Chem.*, 2013, **15**, 3083–3090.
31 M. A. Fuchs, T. A. Zevaco, E. Ember, O. Walter, I. Held, E. Dinjus and M. Doring, *Dalton Trans.*, 2013, **42**, 5322–5329.
32 X. Sheng, L. Qiao, Y. Qin, X. Wang and F. Wang, *Polyhedron*, 2014, **74**, 129–133.
33 A. Buonerba, A. De Nisi, A. Grassi, S. Milione, C. Capacchione, S. Vagin and B. Rieger, *Catal. Sci. Technol.*, 2015, **5**, 118–123.
34 M. Taherimehr, J. P. C. C. Sertã, A. W. Kleij, C. J. Whiteoak and P. P. Pescarmona, *ChemSusChem*, 2015, **8**, 1034–1042.
35 K. L. Collins, L. J. Corbett, S. M. Butt, G. Madhurambal and F. M. Kerton, *Green Chem. Lett. Rev.*, 2007, **1**, 31–35.
36 X. Qian, L. N. Dawe and C. M. Kozak, *Dalton Trans.*, 2011, **40**, 933–943.
37 R. R. Chowdhury, A. K. Crane, C. Fowler, P. Kwong and C. M. Kozak, *Chem. Commun.*, 2008, 94–96.
38 K. Hasan, C. Fowler, P. Kwong, A. K. Crane, J. L. Collins and C. M. Kozak, *Dalton Trans.*, 2008, 2991–2998.
39 R. K. Dean, C. I. Fowler, K. Hasan, K. Kerman, P. Kwong, S. Trudel, D. B. Leznoff, H.-B. Kraatz, L. N. Dawe and C. M. Kozak, *Dalton Trans.*, 2012, **41**, 4806–4816.
40 L. Dyers Jr., S. Y. Que, D. VanDerveer and X. R. Bu, *Inorg. Chim. Acta*, 2006, **359**, 197–203.
41 T. Kurahashi, K. Oda, M. Sugimoto, T. Ogura and H. Fujii, *Inorg. Chem.*, 2006, **45**, 7709–7721.
42 H.-L. Shyu, H.-H. Wei, G.-H. Lee and Y. Wang, *J. Chem. Soc., Dalton Trans.*, 2000, 915–918.
43 R. Mayilmurugan, M. Sankaralingam, E. Suresh and M. Palaniandavar, *Dalton Trans.*, 2010, **39**, 9611–9625.
44 M. Velusamy, M. Palaniandavar, R. S. Gopalan and G. U. Kulkarni, *Inorg. Chem.*, 2003, **42**, 8283–8293.
45 E. F. Chard, J. R. Thompson, L. N. Dawe and C. M. Kozak, *Can. J. Chem.*, 2014, **92**, 758–764.
46 J. B. H. Strautmann, S. D. George, E. Bothe, E. Bill, T. Weyhermüller, A. Stammler, H. Bögge and T. Glaser, *Inorg. Chem.*, 2008, **47**, 6804–6824.
47 P. Mialane, E. Anxolabéhère-Mallart, G. Blondin, A. Nivorojkine, J. Guilhem, L. Tchertanova, M. Cesario, N. Ravi, E. Bominaar, J.-J. Girerd and E. Münck, *Inorg. Chim. Acta*, 1997, **263**, 367–378.
48 R. Viswanathan, M. Palaniandavar, T. Balasubramanian and T. P. Muthiah, *Inorg. Chem.*, 1998, **37**, 2943–2951.
49 M. Merkel, F. K. Müller and B. Krebs, *Inorg. Chim. Acta*, 2002, **337**, 308–316.
50 A. M. Reckling, D. Martin, L. N. Dawe, A. Decken and C. M. Kozak, *J. Organomet. Chem.*, 2011, **696**, 787–794.
51 R. van Gorkum, J. Berding, A. M. Mills, H. Kooijman, D. M. Tooke, A. L. Spek, I. Mutikainen, U. Turpeinen, J. Reedijk and E. Bouwman, *Eur. J. Inorg. Chem.*, 2008, **2008**, 1487–1496.
52 T. N. Rao, J. Reedijk, J. Vanrijn, G. C. Verschoor, A. W. Addison, T. N. Rao, J. Reedijk, J. van Rijn and G. C. Verschoor, *J. Chem. Soc., Dalton Trans.*, 1984, 1349–1356.
53 T. Aida and S. Inoue, *Acc. Chem. Res.*, 1996, **29**, 39–48.

54 M. North and R. Pasquale, *Angew. Chem., Int. Ed.*, 2009, **48**, 2946–2948.
55 M. A. Fuchs, T. A. Zevaco, E. Ember, O. Walter, I. Held, E. Dinjus and M. Döring, *Dalton Trans.*, 2013, **42**, 5322–5329.
56 C. J. Whiteoak, N. Kielland, V. Laserna, E. C. Escudero-Adán, E. Martin and A. W. Kleij, *J. Am. Chem. Soc.*, 2013, **135**, 1228–1231.
57 J. R. Wildeson, J. C. Yarbrough, J. H. Reibenspies, D. J. Darensbourg, J. R. Wildeson, J. C. Yarbrough and J. H. Reibenspies, *J. Am. Chem. Soc.*, 2000, **122**, 12487–12496.
58 J. Rintjema, R. Epping, G. Fiorani, E. Martín, E. C. Escudero-Adán and A. W. Kleij, *Angew. Chem., Int. Ed.*, 2016, 3972–3976.
59 E. Martin, M. Martinez Belmonte, J. Benet-Buchholz, A. W. Kleij, C. J. Whiteoak, M. M. Belmonte and A. W. Kleij, *Adv. Synth. Catal.*, 2012, **354**, 469–476.
60 F. Castro-Gómez, G. Salassa, A. W. Kleij and C. Bo, *Chem. – Eur. J.*, 2013, **19**, 6289–6298.
61 D. J. Darensbourg, J. C. Yarbrough, C. Ortiz and C. C. Fang, *J. Am. Chem. Soc.*, 2003, **125**, 7586–7591.
62 D. Alhashmialameer, N. Ikpo, J. Collins, L. N. Dawe, K. Hattenhauer and F. M. Kerton, *Dalton Trans.*, 2015, **44**, 20216–20231.